Journal of New Results in Science

https://dergipark.org.tr/en/pub/jnrs

Research Article

Open Access

E-ISSN:1304-7981 https://doi.org/10.54187/jnrs.1527152

An investigation of the enzymatic oligomerization of nitro-substituted phenylene diamine: Thermal and fluorescence properties

Feyza Kolcu[1]

Keywords:
p-phenylenediamine, Horseradish peroxidase, Enzyme-catalyzed oligomerization, Green photoluminescence emission, Limiting oxygen index

Abstract — 2-nitro-*p*-phenylenediamine, an aromatic diamine, was studied for its oxidative oligomerization with H_2O_2 using enzyme-catalyzed oligomer synthesis. Characterization of molecular structures was performed utilizing ultraviolet-visible (UV-Vis) spectrophotometer, Fourier-transform infrared spectroscopy (FT-IR), and nuclear magnetic resonance (NMR) techniques, identifying phenazinebridged oligomer resulting from the enzymatic oligomerization process. Based on the results of gel permeation chromatography (GPC) analysis, the synthesized compound was identified as being in an oligomeric form. Conversely, the number of repeating units, as determined by weight average molecular weight (M_w), was found to be 28. The solvent effect on the optical features of the synthesized oligomer in polar solvents was analyzed. The degradation of phenazine-type structures in the oligomer occurred at higher temperatures than that of the monomer. Under visible light excitation, the oligomer exhibited green light emission with a quantum yield (QY) of 6.2% in *N*,*N*-dimethylformamide (DMF). 2-nitro-*p*-phenylenediamine was readily oxidized into an oligomer with *ortho*-coupled constitutional units, having a lower electrochemical band gap than the monomer, via the enzymatic oligomerization route. Scanning electron microscopy revealed that enzyme-catalyzed oxidation of monomers exhibited a spongy morphology with some pores.

Subject Classification (2020): 80A50, 82D60

1. Introduction

π-conjugated polymers, particularly polyaniline and its derivatives have garnered significant interest in developing advanced materials. Among these, polyphenylenediamines are notable as important conducting polymers due to their facile synthesis. Aromatic diamine polymers offer unique functionalities compared to polyanilines, making them promising for applications in electrochromism and electrochromic cells [1,2]. The aromatic units within the conjugated polymer main chains, structured by an sp^2 carbon framework, facilitate charge transport along the polymer backbones [3,4]. Therefore, synthesizing novel conjugated polymers is crucial for technological applications [5,6]. Conducting polymers like polyaniline (PANI) and its derivatives are highly regarded for their well-defined structure and distinctive electrical and optical features [3]. PANI and poly(phenylenediamine) have seen increasing interest as polymeric adsorbents for heavy metals and various dyes due to their environmental stability [7].

Aromatic diamines are highly susceptible to oxidative oligomerization/polymerization, which can involve the oxidation of one or both -NH_2 units, forming ladder poly(phenazine) or poly(aminoaniline). These polymers exhibit distinct features compared to other conducting polymers like polyaniline. Poly (*p*-aminoaniline) is only

[1]feyzakolcu@comu.edu.tr (Corresponding Author)
[1]Department of Chemistry and Chemical Processing Technologies, Çanakkale Onsekiz Mart University, Çanakkale, Türkiye
Article History: Received: 02 Aug 2024 — Accepted: 30 Aug 2024 — Published: 31 Aug 2024

slightly soluble in most organic solvents, and its molecular weight is typically in the range of thousands, which is more characteristic of oligomers rather than polymers. These polymers can improve solubility by introducing polar side groups like NO_2 substituents [8].

From the perspective of oligomer/polymer mechanisms, enzymatic polymer synthesis is a crucial aspect of green polymer chemistry [9]. Horseradish peroxidase (HRP) facilitates the decomposition of H_2O_2 and catalyzes the oxidative oligomerization/polymerization of aromatic amine derivatives [10]. Enzymes are highly effective catalysts for synthesizing macromolecules, operating under mild reaction conditions. Amine functional groups act as initiators for various crosslinking reactions, essential in forming plastic thermosets, adhesives, and biologically active substances [11].

This study researched synthesizing and characterizing the enzymatically oligomerized 2-nitro-*p*-phenylenediamine (monomer) compound. The study provides insights into designing structures to improve the solubility of nitro-bearing oligomers. The synthesized oligomer exhibited green light emission upon visible light excitation. In the enzyme-catalyzed oxidative oligomerization of 2-nitro-*p*-phenylenediamine, the oxidation of *p*-phenylenediamine produces cationic radicals, leading to the formation of *ortho*-coupled or head-to-tail units via N-C linkage formation, culminating in oligomer. Konyushenko et al. suggested that phenazine units play a part in gathering polyaniline-related nanostructures [12]. The study aimed to elucidate the feasibility of an enzyme-catalyzed oligomerization mechanism for 2-nitro-*p*-phenylenediamine. Comparative analyses were conducted using photoluminescence (PL), thermogravimetric analysis (TGA), ultraviolet-visible (UV-Vis) spectrophotometer, differential scanning calorimetry (DSC), and cyclic voltammograms (CV) techniques to evaluate the oligomer's photoluminescence, thermal, and electrochemical features.

2. Materials and Methods

2.1. Materials

Horseradish Peroxidase (HRP) and 2-nitro-*p*-phenylenediamine (monomer) were procured from Sigma-Aldrich Chemical Co. and Across Organics, respectively. Additionally, Sigma-Aldrich Chemical Co. provided ethanol (EtOH), methanol (MetOH), dimethyl sulfoxide (DMSO), acetonitrile (CH_3CN), dichloromethane (CH_2Cl_2), tetrahydrofuran (THF), heptane, hexane, 1,4-dioxane, *N*,*N*-dimethylformamide (DMF), Tetrabutylammonium hexafluorophosphate (NBu_4PF_6), pH=7 disodium hydrogen phosphate, and 35% hydrogen peroxide (H_2O_2). No further purification was needed for the chemicals used as received.

2.2. Enzymatic oligomerization of 2-nitro-*p*-phenylenediamine

A mixture of monomer (2.0 mmol, 0.306 g) and 5 mg of HRP was prepared in 30 mL of 1,4-dioxane, comprising 0.1 M disodiumhydrogen phosphate buffer solution (10 mL). The enzymatic oligomerization was commenced by putting in 230 µL of H_2O_2. Subsequently, 1 mL of H_2O_2 was added in 1 hour at room temperature. After approximately 24 hours, a dark brown precipitate formed at the bottom of the flask, indicating a successful oligomerization at room temperature. The resulting product was filtered to remove unreacted reactants, which were washed away with 100 mL of distilled H_2O three times. Drying the oligomer was performed in a vacuum oven at 45 °C, yielding 61%. The suggested mechanism for the oligomer formation is outlined in Scheme 1.

2.3. Instruments

The solubility test was conducted with 1 mg of oligomer, thoroughly dispersed in 1 mL of solvent. The functional groups of the monomer and oligomer were analyzed using a PerkinElmer FT-IR Spectrum One, including an ATR accessory, covering the range 4000-400 cm^{-1}. With DMSO-d_6 and tetramethylsilane (TMS), ^1H and ^{13}CNMR spectra were obtained using an Agilent 600 MHz and 150 MHz Premium COMPACT NMR Magnet, respectively. The molecular weight distribution of the oligomer was specified using Gel Permeation

Chromatography (GPC) with Light Scattering and Refractive Index detectors (Malvern Viscotek GPC Dual 270 max). The GPC column was calibrated at 55 ºC, using polystyrene standards (162-60.0000 Dalton (Da), Polymer Laboratories).

DMF containing 40 mM lithium bromide (LiBr) was used as the mobile phase. The optical features of the monomer and its oligomer were assessed using an Analytikjena Specord 210 spectrometer in the wavelength range of 280-700 nm. The measurements were conducted using sample solutions placed in a 1 cm quartz cell. Photoluminescence (PL) measurements were performed by a Shimadzu RF-5301PC spectrofluorophotometer (slit width: 5 nm). Thermogravimetric-Differential Thermal Analysis (TG-DTA) was performed using Perkin Elmer Diamond Thermal Analyzer from 25 °C to 1000 °C. Differential Scanning Calorimetry (DSC) analysis was performed using a Perkin Elmer Sapphire Differential Scanning Calorimeter between 25 °C and 420 °C (N_2 atmosphere and heating rate: 10 °C min^{-1}). A CHI 660C Electrochemical Analyzer was used to monitor CV with a 25 mV s^{-1} scan rate. The measurements under argon employed a cell consisting of a silver and a platinum wire as a reference and auxiliary electrode, respectively, as well as a GCE as a working electrode, in a 0.1 M NBu_4PF_6 in CH_3CN solution as the supporting electrolyte. The band gap ($E_g^{'}$) between the electrochemical highest occupied molecular orbital - lowest unoccupied molecular orbital (HOMO-LUMO) levels and were obtained from the cyclic voltammograms [13]. Scanning Electron Microscopy (SEM) photographs were received to analyze the morphology of the oligomeric particles.

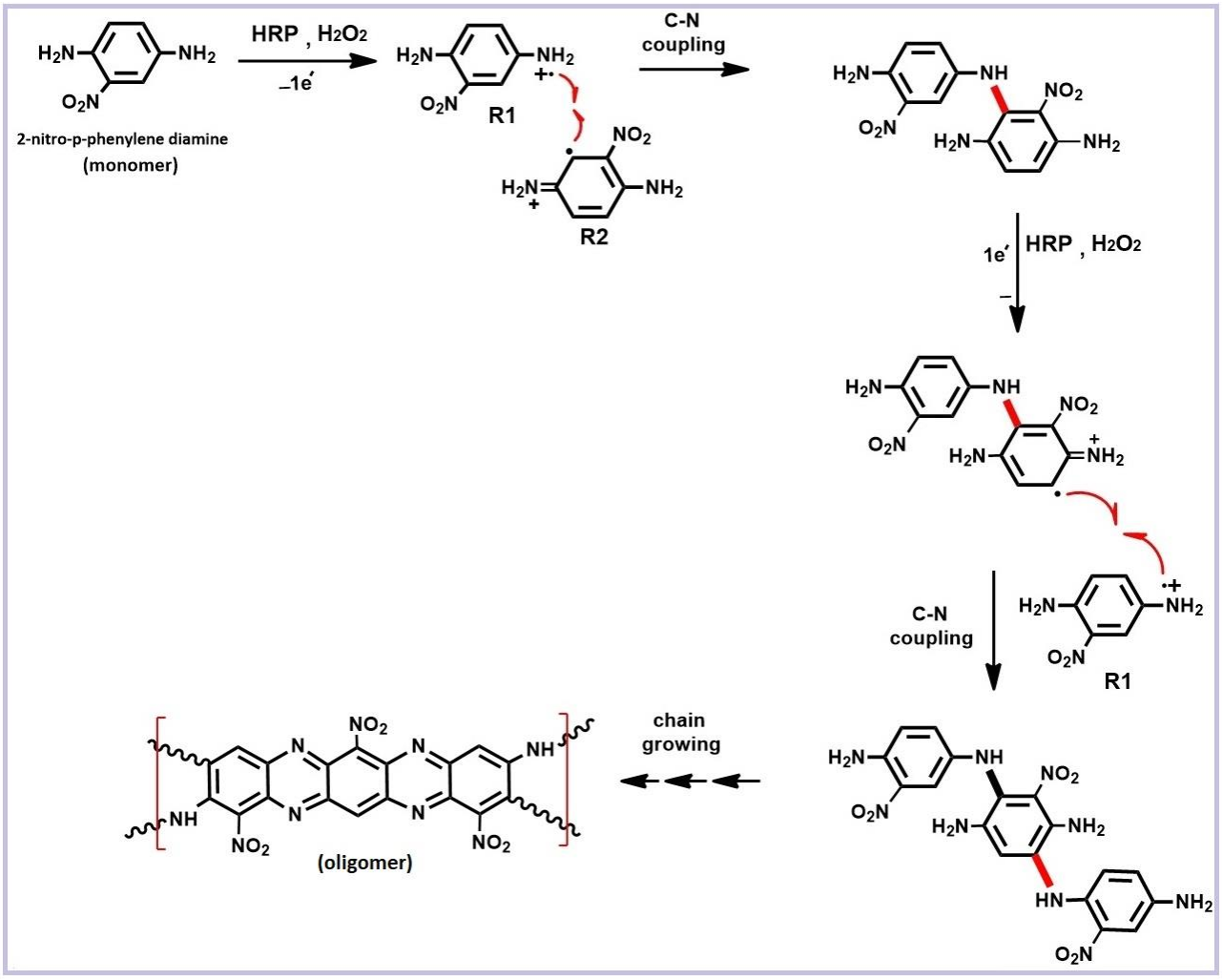

Scheme 1. Synthesis procedure for the oligomer

3. Results and Discussion

3.1. Spectral Comments on Monomer and Oligomer

2-nitro-*p*-phenylenediamine was enzymatically oligomerized, as shown in Scheme 1. The yield of brown-colored oligomer was 51%. Fine solubility of the oligomer in MetOH, EtOH, DMSO, DMF, CH_2Cl_2, and CH_3CN was observed, whereas it was insoluble in apolar solvents, such as heptane and hexane.

The coupling of R1 and R2 radicals resulted in the formation of the enzyme-catalyzed oligomer. Two monomer radicals were coupled to initiate the chain extension of the oligomer. R1 and R2 have the potential to interact, forming a concurrent double C-N-C bond because of intramolecular oxidative cyclization, leading to the formation of phenazine units in a ladder-type oligomer (Scheme 1) [14].

Figure 1 presents the FT-IR spectra of the monomer and its enzymatically oligomerized product. The N-H stretching wavenumbers observed at 3440 and 3326 cm^{-1}, corresponding to the primary amine groups in monomer, were detected at 3466 and 3366 cm^{-1} for oligomer. The peaks at 3455 and 3359 cm^{-1}, associated with the N-H stretching modes, indicate the presence of NH-/-NH_2 in the oligomer. The C-H stretching modes of monomer and oligomer were displayed at 3170 and 3179 cm^{-1}, respectively. The N-H bending vibration of primary amine in the monomer was observed at 1591 cm^{-1}. The C=C stretching of the monomer was noticed within the range of 1568 to 1513 cm^{-1}. The stretching mode of C=N in the phenazine unit showed itself as an appearing peak at 1630 cm^{-1} in the oligomer's spectrum [14]. The asymmetrical and symmetric N-O stretching bands were monitored at 1475 and 1334 cm^{-1} and 1475 and 1331 cm^{-1}, respectively. Additionally, bands at 820 at 826 cm^{-1} are related to ring hydrogen deformation vibrations.

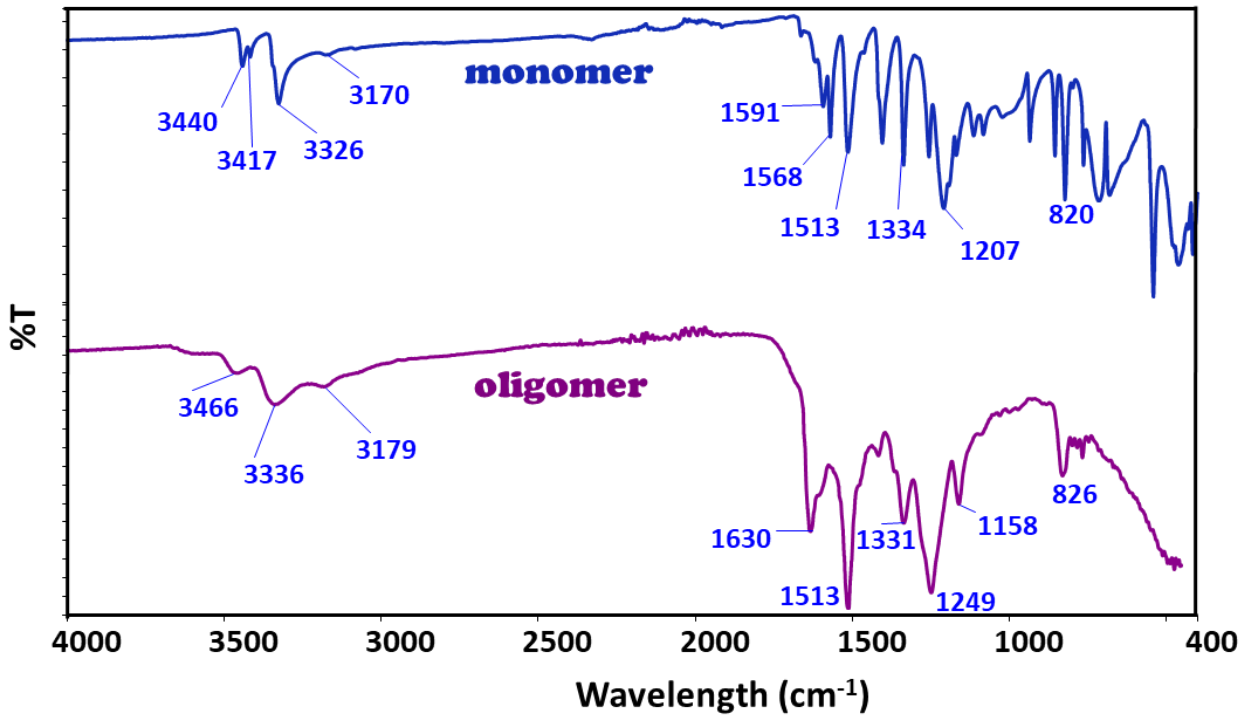

Figure 1. FT-IR spectra of monomer and oligomer

^{1}H NMR spectra of the monomer and its oligomer were analyzed to elucidate their molecular structures, as shown in Figure 2. For the monomer, the peaks at 4.80 (singlet), 6.81 (doublet), 6.86 (doublet), and 7.11 (singlet) ppm were related to three aromatic hydrogen protons and four amino hydrogens, respectively, as seen in Figure 2A. The *ortho*-coupled monomer units underwent intramolecular cyclization, forming a phenazine-type structure. The transformation of primary to secondary amine via N-C coupling is evidenced by the appearance of a singlet at 7.88 ppm, as depicted in Figure 2B. The terminal -NH_2 groups were ascribed to the peak at 6.94 ppm.

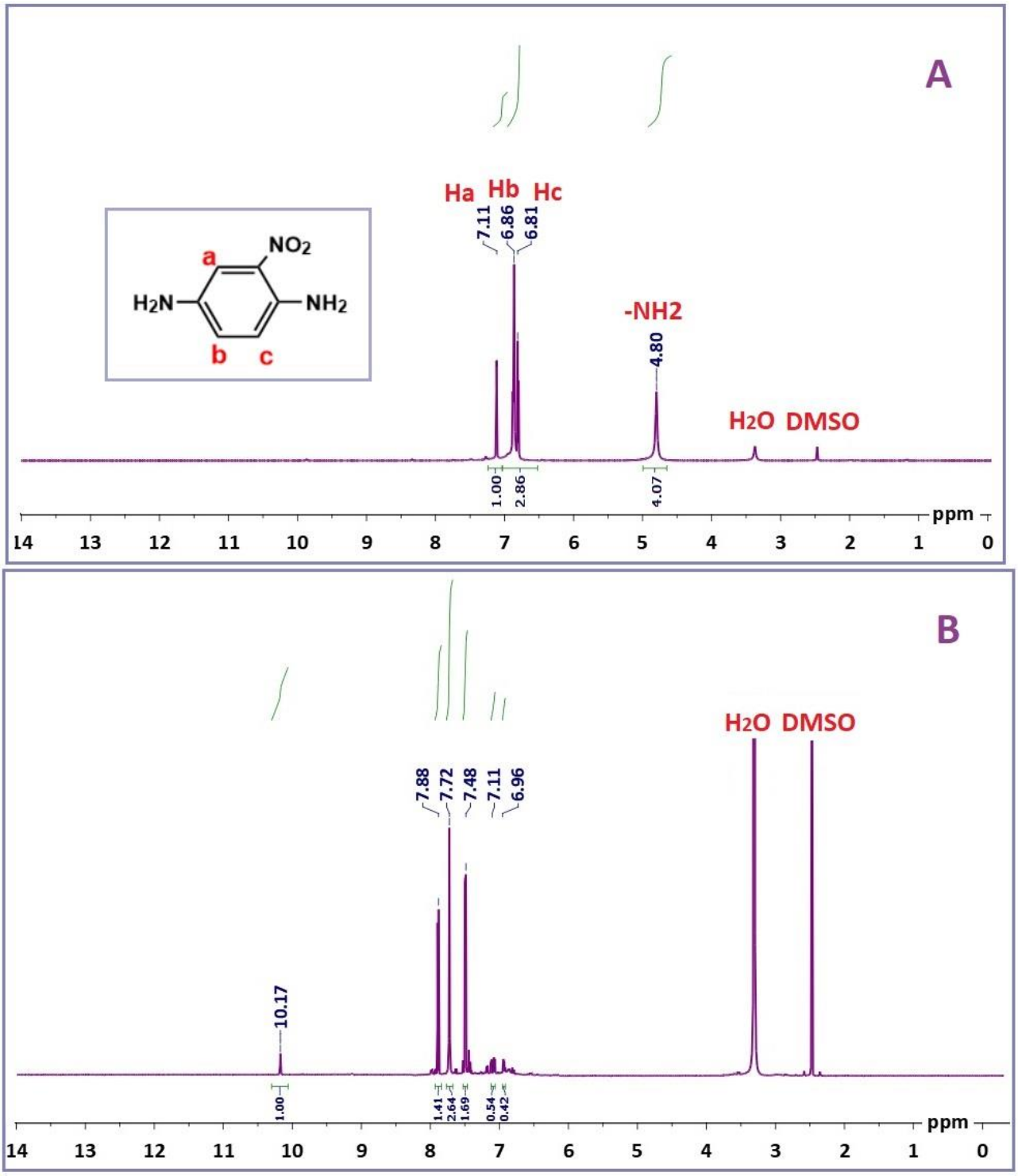

Figure 2. [1]H NMR spectra of (A) monomer and (B) oligomer

[13]C NMR spectrum of the monomer indicated the signals for C1, C3, and C4, which carry -NH_2, -NO_2, and -NH_2, appearing at downfield shifts of 139.65, 138.98, and 130.67 ppm, respectively, as seen in Figure 3A. Due to the +M effect of NH_2 groups, the carbon signals of C6, C5, and C2 at the *ortho* position shifted upfield at 127.53, 120.33, and 105.72 ppm, respectively. According to Figure 3B, two distinct peaks at 160.02 and 150.62 ppm could be evidence of two C=N bonds due to the phenazine ring formation in the enzyme-catalyzed oligomerization.

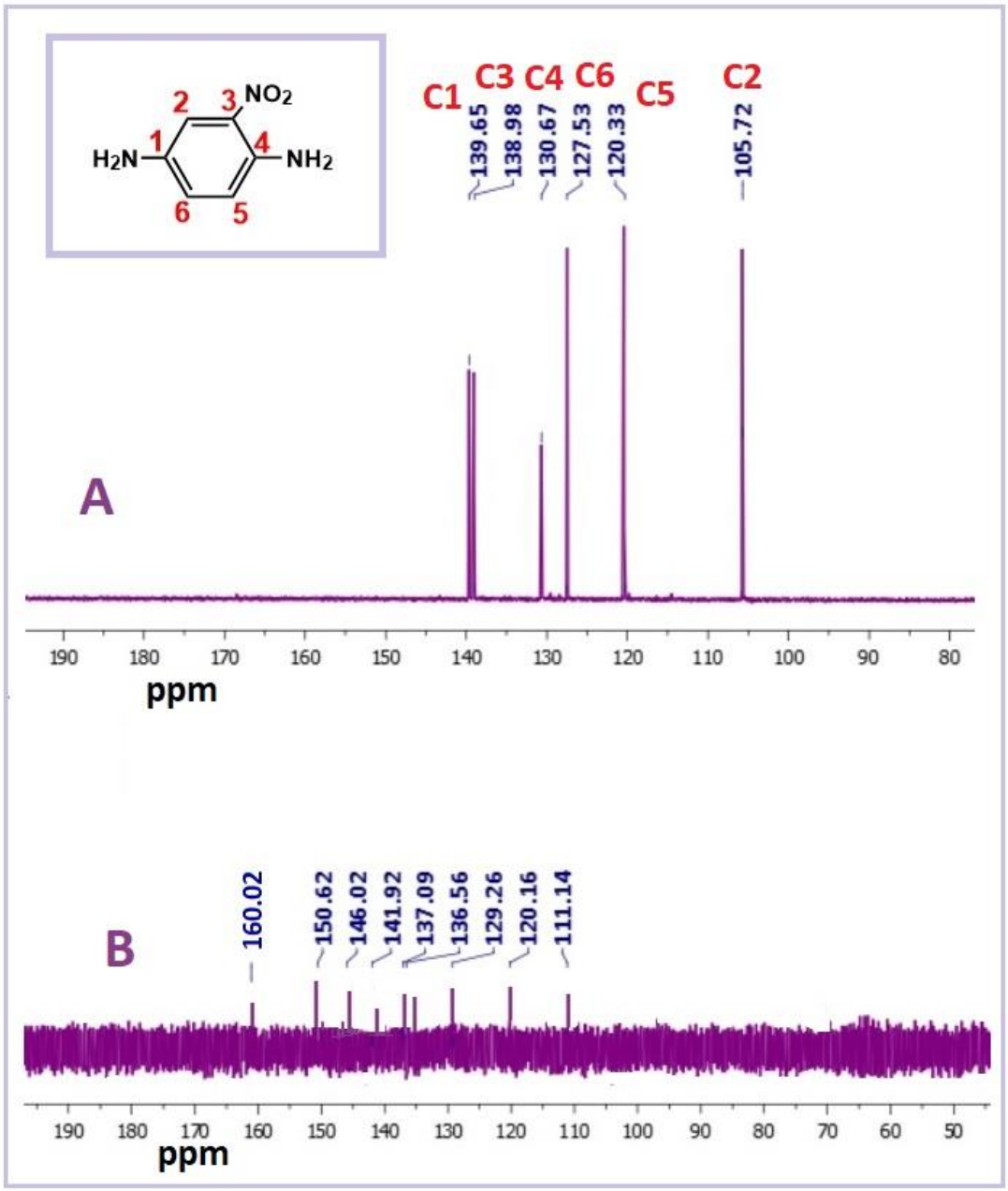

Figure 3. ^{13}C NMR spectra of (A) monomer and (B) oligomer

Based on the GPC analysis of the oligomer, weight average molecular weight (M_w) and number average molecular weight (M_n) were found to be 4350 and 3800 Da, respectively, confirming that the synthesized compound possesses an oligomeric structure. PDI value, calculated as the ratio of M_w to M_n, was determined as 1.14. Based on M_w and M_n, the average number of repeating units was 28 and 25, respectively.

3.2. Electrochemical and Optical properties

Due to phenazine units appearing in the enzymatic oligomerization, the π→π* electronic transition for the oligomer was observed between 280 and 348 nm. The synthesized oligomer's UV-vis properties were analyzed and presented in Figure 4 to investigate the solvent effect. A broad signal, ascribed to the n→π* electronic transition of NH_2 and NO_2 groups, was detected in the 400-600 nm range. The π→π* electronic transition in the oligomer remained unaffected by changing the solvent polarity. The maximum absorption wavelength (λ_{max}) values of the oligomer were observed to be 474 nm, 476 nm, 482 nm, 483 nm, 488 nm, and 493 nm in CH_2Cl_2, CH_3CN, MetOH, EtOH, DMF, and DMSO, respectively, indicating a bathochromic shift of n→π* band as the solvent polarity increased, as seen in Figure 4.

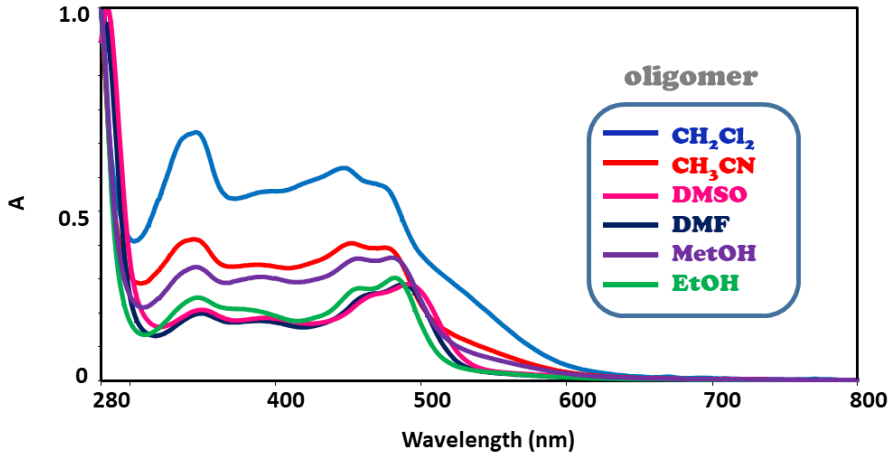

Figure 4. Normalized UV-vis spectra of enzyme-catalyzed oligomer in solvents.

Protic solvent molecules orient themselves around the chromophore of the oligomer, forming hydrogen bonds with the unshared electron pairs on the oxygen and nitrogen atoms. Upon establishing the intermolecular hydrogen bonding, the energy gap between the HOMO and the LUMO levels decreases with increasing solvent polarity, leading to a shift of (λ_{max}) towards longer wavelengths. The π→π* transition in the aromatic moiety of the oligomer remains unaffected by the solvent.

The peaks for oxidation and reduction potentials of the compounds are determined using Cyclic Voltammograms, as presented in Figure 5. During oxidation, one electron is removed from the HOMO level. A radical cation, generated through CV oxidation, subsequently underwent a radical-radical coupling related to deprotonation, forming a dimer [15]. The anodic peaks can be ascribed to the oxidation of -NH_2 of monomer and oligomer, forming a polaron structure ($^{\bullet+}$NH) through coupling with the parent molecule. Following the formation of the oligomer, the terminal amino groups undergo oxidation due to their lower oxidation potentials.

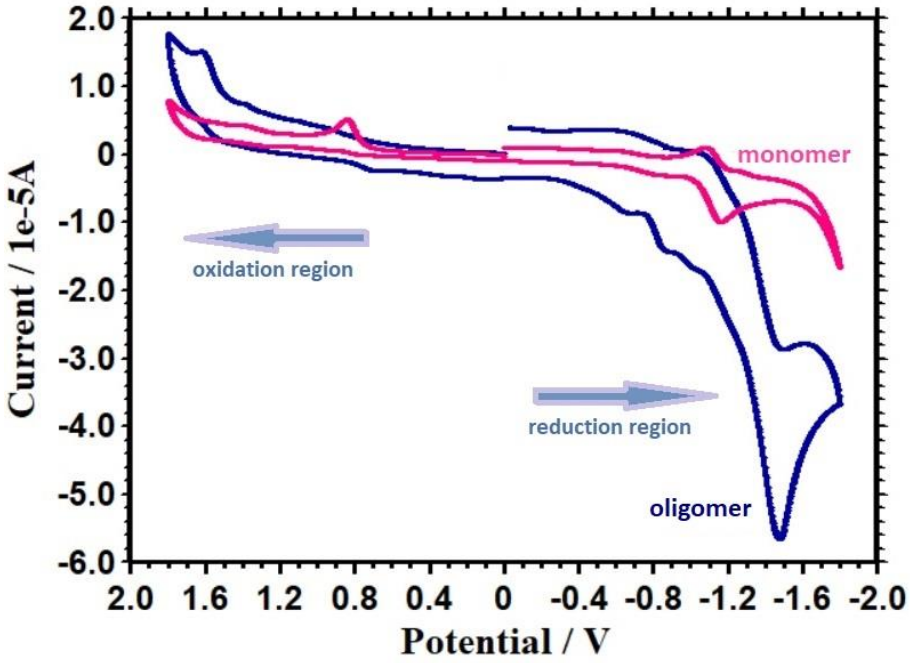

Figure 5. CVs of monomer and oligomer

The -C=N- group exhibits high sensitivity to reduction in the synthesized oligomer. During the negative scan, the -C=N- group undergoes reduction at -1471 mV. The elevation of HOMO from -5.58 V to -5.87 V and the reduction of the LUMO from 2.97 V to 3.01 V during the oligomer formation was observed. The enzyme-catalyzed oligomer had a lower $E_g^{'}$ values than monomer.

3.3. Fluorescence (PL) Characteristics

The PL spectrum of the obtained oligomer was recorded to study its photoluminescence property. Green light emission was observed in DMF for the enzyme-catalyzed oligomer, as presented in Figure 6. The maximum emission wavelength (λ_{max}) occurred at 507 nm, corresponding to the emission of green light when excited by 410 nm. Fluorescent light emission intensity was measured at 410 a.u. PL characteristics could be attributed to quantum yield (QY) [16]. The oligomer synthesized enzymatically exhibited QY of 6.2% for green photoluminescence emission. Notably, the enzyme-catalyzed oligomer, synthesized using an environmentally friendly method, appears promising for future development in optoelectronic devices. The inset displays the time-dependent (0-3600 s) fluorescence measurement under 410 nm light excitation. No changes in fluorescence intensity were observed over 3600 s under identical conditions, indicating that the enzymatically synthesized oligomer exhibits excellent photostability when excited by 410 nm light. Consequently, the synthesized oligomer shows promising potential for producing display devices and light-emitting diodes.

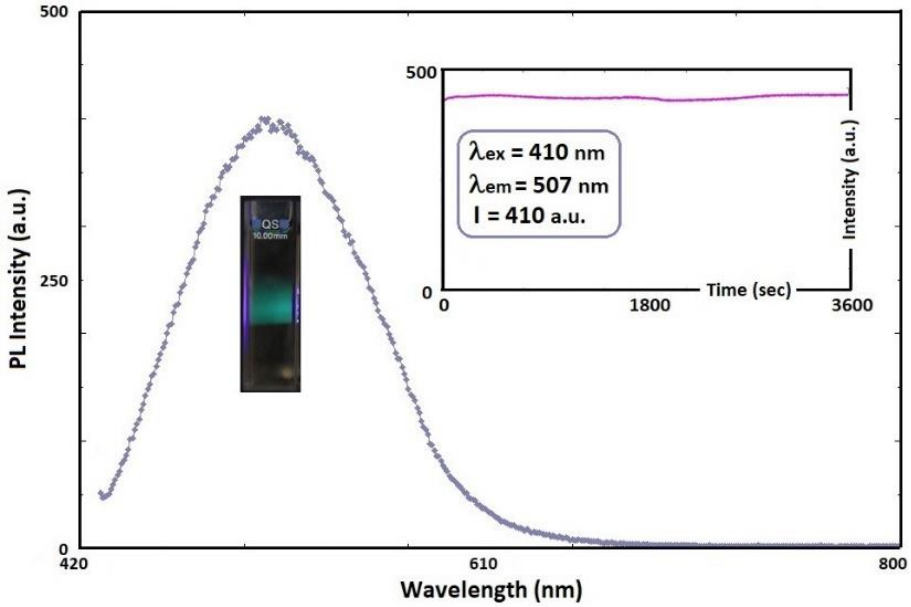

Figure 6. PL emission spectrum of oligomer Inset: Time-dependent PL spectrum of oligomer

3.4. Thermal Stability

The thermal properties of the monomer and the synthesized oligomer were investigated using TGA-DTG instruments from 25 °C to 1000 °C, as presented in Figure 7. The thermal degradation of the monomer and oligomer occurred in two steps, as noticed in Figure 7. Although solvent evaporation was not observed in the monomer, it was evident in the synthesized oligomer as an initial weight loss of 9.30% from 30 °C to 120 °C, attributed to the moisture trapped within the oligomer chains. The degradation (T_{on}) of the monomer and oligomer started at 231 and 310 °C, respectively. The oligomer's higher T_{on} value than the monomers can be explained by the conjugation resulting from the linkage of monomer units via phenazine formation, as depicted in Scheme 1.

Consequently, the phenazine-type structures' degradation within the oligomer occurs at higher temperatures than the monomer (Figure 7A). The maximum weight loss (T_{max}) occurred for the monomer and oligomer were 266 °C and 796 °C, and 329 °C and 751 °C, respectively, as observed in Figure 7B. Furthermore, the temperatures corresponding to 20% weight loss (T_{20}) and 50% weight loss (T_{50}) were found at 259 °C and 331 °C for the monomer and 341 °C and 728 °C for the oligomer, respectively.

The monomer decomposition occurred between 150 °C and 417 °C, resulting in a 52.18% weight loss, and continued to 1000 °C with an additional 18.40% weight loss. For the oligomer, two decomposition stages were

observed: the first ranged from 110 °C to 377 °C with a 31.14% weight loss, and the second stage ranged from 377 °C to 1000 °C with a 36.82% weight loss. The char% was calculated to be 28.93% for the monomer and 33.04% for the oligomer. This residual content is attributed to the decomposition of the oligomer's rigid chain structure, organized into a structural order stabilized by phenazine units. T_{max} values indicate that the thermal steadiness of the synthesized oligomer is superior to that of the monomer. Therefore, the synthesized oligomer demonstrates the potential for applications across diverse industrial sectors, including electrical applications necessitating high-temperature insulation in manufacturing aircraft components, weapon systems, and space vehicles [11].

The flame retardancy value of the oligomer can be obtained using the TGA curve following Van Krevelen's calculation, utilizing the percentage of residue at 1000 °C. The formation of carbon during thermal decomposition restricts the emission of organic volatile compounds. This carbonaceous layer, produced in the process, impedes the propagation of flammable gases by diminishing heat transfer to the material. In this regard, Van Krevelen proposed a formula of LOI = 17.5 + 0.4 (*s*) where LOI represents the limiting oxygen index and (*s*) denotes the percentage of residue in the polymer, respectively [17]. According to Van Krevelen's theory, an increase in residue formation correlates with the flammability of polymers. For polymers to be self-extinguishing, their LOI values must be at least 26 or higher [18]. The LOI value of the synthesized oligomer was calculated as 30.72, indicating that the oligomer exhibits excellent thermal stability and lower flammability. From DSC measurements, the glass transition temperature (T_g) and specific heat capacity (ΔC_p) values of the oligomer were calculated to be 208 °C and 0.384 J/g °C, respectively. An exothermic peak at 340 °C was observed in the DSC curve of the oligomer.

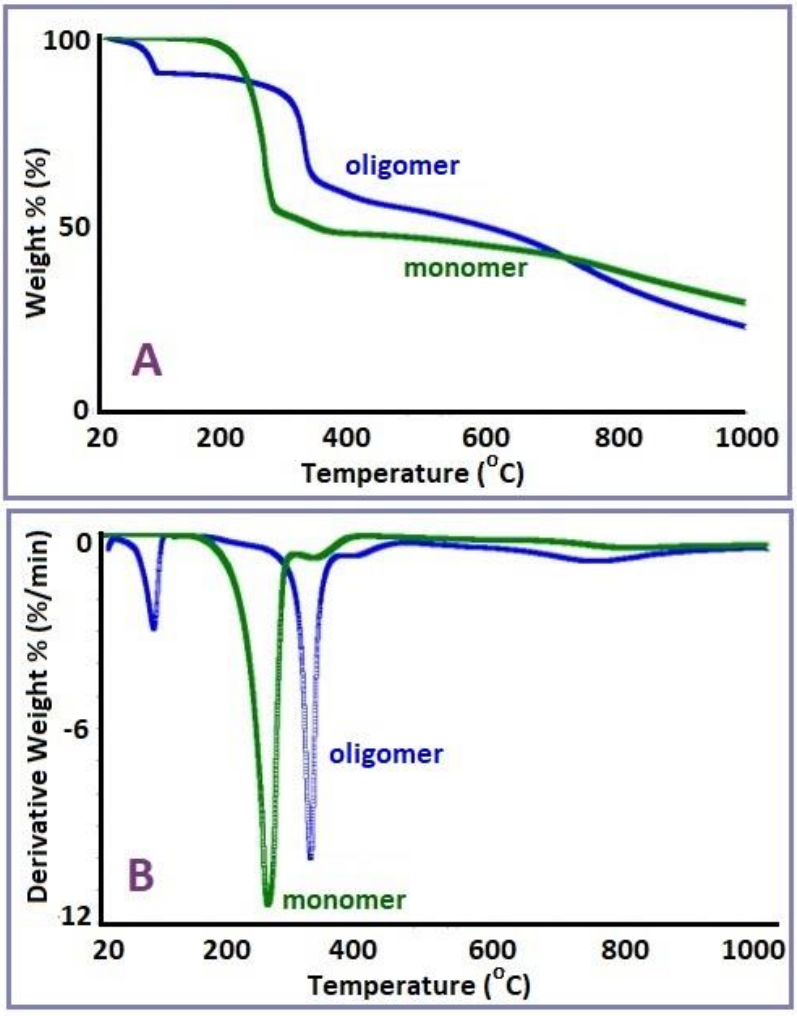

Figure 7. (A) TGA and (B) DTG curves of monomer and its oligomer

3.5. Morphological Properties

The sample was sprinkled onto the stub and subsequently subjected to a sputter coating with a 5 nm layer of gold. Morphological properties of the enzyme-catalyzed oligomer were examined using SEM at different magnifications, as illustrated in Figure 8. As depicted in Figure 8, the surface morphology of the oligomer exhibited a sponge-like structure with an irregular network. The accumulated oligomer particles formed a dense, shrunken mass with a rough surface.

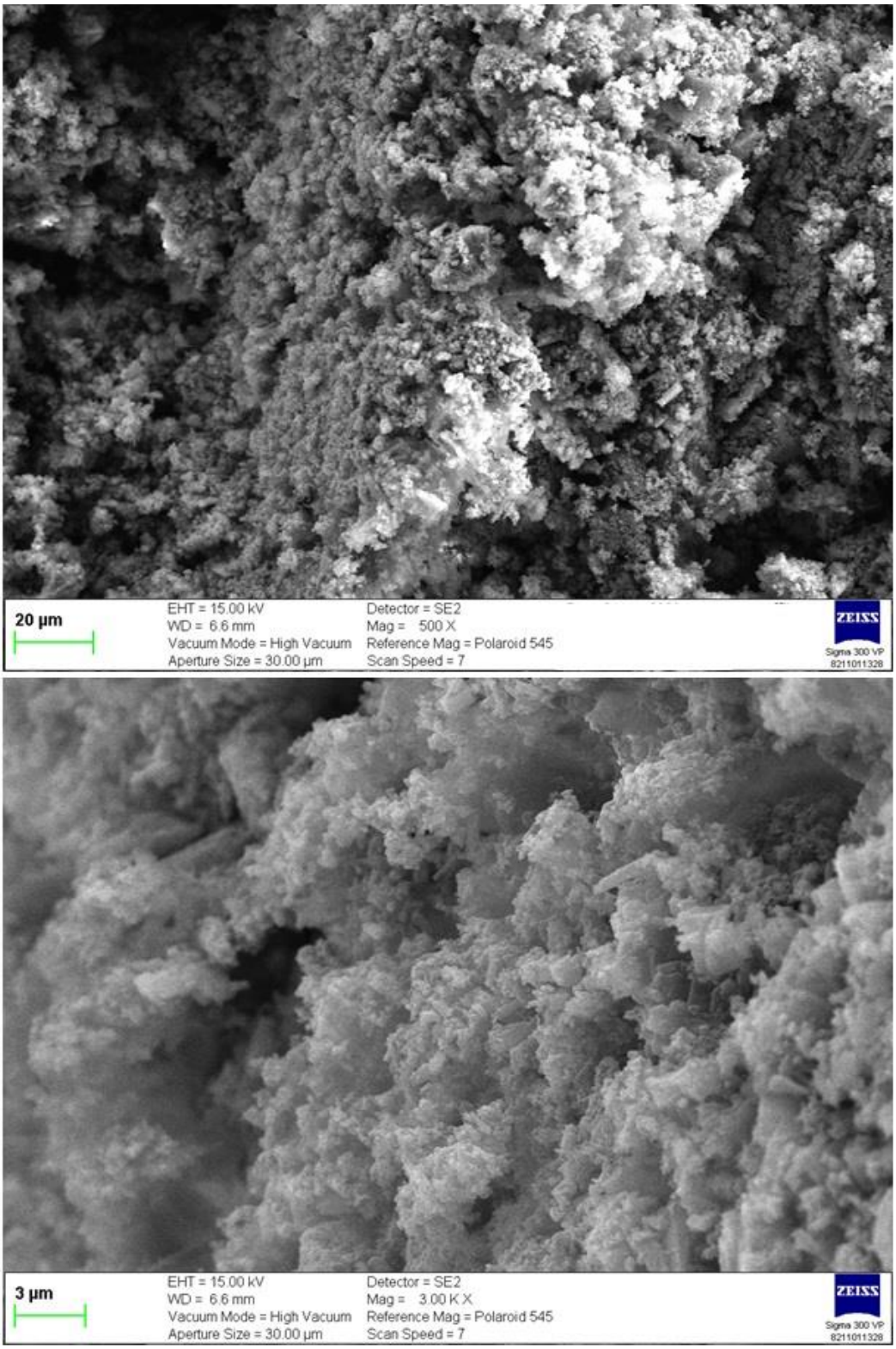

Figure 8. SEM views of the oligomer

4. Conclusions

The oxidation of 2-nitro-*p*-phenylenediamine, an aromatic diamine compound, resulted in an enzyme-catalyzed oligomer. The solvent's polarity significantly influenced the synthesized oligomer's UV-vis absorption. Due to its potential as a green light emitter, the enzyme-catalyzed oligomer can be a promising compound for the fabrication of display devices and applications in bioscience. Additionally, the exceptional thermal stability of the oligomer suggested its suitability for use in the manufacture of electrical appliances requiring high-temperature insulation. These attributes highlighted the advantages of the enzymatic synthetic process, which provides simplicity in synthesis, environmental compatibility, chemical stability, and notable thermal and photophysical features. Obtaining and characterizing macromolecules using different catalysts and oxidative polymerization methods for the monomer used in this study will shed light on future studies.

Author Contributions

The author read and approved the final version of the paper.

Conflict of Interest

The author declares no conflict of interest.

Ethical Review and Approval

No approval from the Board of Ethics is required.

References

[1] T. Qin, L. Deng, P. Zhang, M. Tang, C. Li, H. Xie, S. Huang, X. Gao, *Enhancement of Electrochromic Properties of Polyaniline Induced by Copper Ions*, Nanoscale Research Letters 17 (2022) Article Number 51 13 pages.

[2] K. Chiba, T. Ohsaka, N. Oyama, *Electrode kinetics of electroactive electropolymerized polymers deposited on graphite electrode surfaces*, Journal of Electroanalytical Chemistry and Interfacial Electrochemistry 217 (2) (1987) 239-251.

[3] G. E. J. Garion, S. Li, N. K. Obhi, C. N. Jarrett-Wilkins, D. S. Seferos, *Programmable assembly of π-conjugated polymers*, Advanced Materials 33 (46) (2021) Article Number 2006287 21 pages.

[4] M. Li, X. Zhang, S. Zhen, J. Xu, *Multichannel transport in conjugated polymers based on through-space conjugated naphthalene*, New Journal of Chemistry 45 (2021) 1795-1799.

[5] A. Khosravi, M. Vossoughi, S. Shahrokhian, Iran Alemzadeh, *HRP-dendron nanoparticles: the efficient biocatalyst for enzymatic polymerization of poly (2,5-dimethoxyaniline)*, Journal of Molecular Catalysis B: Enzymatic 90 (2013) 139-143.

[6] A. Douka, S. Vouyiouka, L. M. Papaspyridi, C. D. Papaspyrides, *A review on enzymatic polymerization to produce polycondensation polymers: the case of aliphatic polyesters, polyamides and polyester amides*, Progress in Polymer Science 79 (2018) 1-25.

[7] I. Sapurina, J. Stejskal, *The mechanism of the oxidative polymerization of aniline and the formation of supramolecular polyaniline structures*, Polymer International 57 (12) (2008) 1295-1325.

[8] X. G. Li, X. L. Ma, J. Sun, M. R. Huang, *Powerful reactive sorption of Silver(I) and Mercury(II) onto Poly(o-phenylenediamine) microparticles*, Langmuir 25 (2009) 1675-1684.

[9] A. G. El-Shekeil, H. A. Al-Saady, F. A. Al-Yusufy, *Synthesis and characterization of some soluble conducting polyazomethine polymers*, Polymer International 44 (1) (1997) 78-82.

[10] S. Kobayashi, A. Makino, *Enzymatic polymer synthesis: An opportunity for green polymer chemistry*, Chemical Reviews 109 (11) (2009) 5288-5353.

[11] P. Xu, A. Singh, D. L. Kaplan, *Enzymatic catalysis in the synthesis of polyanilines and derivatives of polyanilines*, in: S. Kobayashi, H. Ritter, D. Kaplan (Eds), Enzyme-Catalyzed Synthesis of Polymers, Vol 194 of Advances in Polymer Science, Springer, Berlin, Heidelberg, 2006, pp. 69-94.

[12] E. N. Konyushenko, J. Stejskal, I. Šeděnková, M. Trchová, I. Sapurina, M. Cieslar, J. Proke, *Polyaniline nanotubes: conditions of formation*, Polymer International 55 (1) (2006) 31-39.

[13] R. Cervini, X. C., Li, G. W. C., Spencer, A. B., Holme, S. C. Moratti, R. H. Friend, *Electrochemical and optical studies of PPV derivatives and poly(aromatic oxadiazoles)*, Synthetic Metals 84 (1997) 359-360.

[14] L. L. Wu, J. Luo, Z. H. Lin, *Spectroelectrochemical studies of poly-o-phenylamine. Part 1. In situ resonance Raman spectroscopy*, Journal of Physical Chemistry B 112 (23) (2008) 6976-6987.

[15] H. Yang, D. O. Wipf, A. J. Bard, *Application of rapid scan cyclic voltammetry to a study of the oxidation and dimerization of N,N-dimethylaniline in acetonitrile*, Journal of Electroanalytical Chemistry 331 (1-2) (1992) 913-924.

[16] A. T. R. Williams, S. A. Winfield, J. N. Miller, *Relative fluorescence quantum yields using a computer-controlled luminescence spectrometer*, Analyst 108 (1290) (1983) 1067-1071.

[17] D. W. van Krevelen, *Some basic aspects of flame resistance of polymeric materials*, Polymer 16 (8) (1975) 615-620.

[18] İ. Kaya, R. E. İriş, H. K. Yağmur, *Synthesis and characterization of cage structured flame-resistant melamine and pentaerythritol based polymer networks*, Journal of Polymer Research 30 (2023) Article Number 388 15 pages.